Chapter 7

The Importance of the Assembly in Thermoelectric Generators

Miguel Araiz, Leyre Catalan, Oscar Herrero,
Gurutze Perez and Antonio Rodriguez

Additional information is available at the end of the chapter

http://dx.doi.org/10.5772/intechopen.75697

Abstract

Generally, in the optimization of thermoelectric generators, only the heat exchangers or the thermoelectric modules themselves are taken into account. However, the assembly of the generator as a whole is of vital importance since a bad contact or a thermal bridge can waste the performance of an optimal generator. In this sense, the present chapter analyzes experimentally the use of different interface materials to reduce the thermal contact resistance between the modules and the heat exchangers, the influence of the pressure distribution in the assembly as well as the effect of different insulating materials in order to reduce the thermal bridge between the exchangers. Thus, it has been demonstrated that a good assembly requires the implementation of thermal interface materials to ensure the microscopic contact between the heat exchangers and the modules, besides a uniform clamping pressure. Nevertheless, since this is normally achieved with screws, they represent a source of thermal bridges in conjunction with the small distance between the exchangers. In order to reduce heat losses due to thermal bridges, which can represent up to one-third of the incoming heat, an increment of the distance between the exchangers and the use of an insulator is recommended.

Keywords: assembly, pressure distribution, clamping pressure, contact, thermal bridge, thermoelectric generator, thermal resistance

1. Introduction

Thermoelectric generators represent a reliable, robust and compact way for directly converting heat into electricity, as their spread use for space applications demonstrates [1]. However, these devices are hampered by their low efficiency, which has limited their expansion to civil applications.

In order to improve the efficiency of thermoelectric generators, the most common trend focuses on thermoelectric modules, the principal element of the generators since the transformation of heat into electricity is held on them thanks to Seebeck effect. A conventional module is made up of various thermocouples connected electrically in series in order to increase the operating voltage, and thermally in parallel to increase the thermal conductance. Each couple itself is typically composed of two semiconductor thermoelements (an n-type one, in which free electrons predominate, and a p-type one, dominated by free holes) united by a metal conductor. Two rigid substrates of ceramic material provide mechanical firmness to the whole system and isolate the internal circuit.

The efficiency of a thermocouple is proportional to the temperature difference among its sides, as well as to the figure of merit Z (Eq. (1)), which is a function of the Seebeck coefficients α, the thermal conductivities λ and the electrical resistivities ρ of the semiconductors that make up the thermocouple [2].

$$Z = \frac{(\alpha_p - \alpha_n)^2}{\left((\lambda_p \cdot \rho_p)^{1/2} + (\lambda_n \cdot \rho_n)^{1/2}\right)^2} \tag{1}$$

Hence, since efficiency is directly related to the capability of the materials as energy converters, there is a deep research about materials that present an equilibrium between a figure of merit as high as possible and ease of manufacturing [3–7]. Currently available thermoelectric materials present a ZT of around 1 or less, but the outlook for laboratories is to develop materials with a ZT of 2 in order to have an efficiency over 10% and become competitive with other technologies [8]. Nevertheless, this is not an easy task since the three parameters that define Z closely depend on one another [9]. Bismuth-telluride (Bi2Te3), half Heusler, skutterudites, oxides, magnesium silicides and tetrahedrites are the materials already available commercially [8].

Nonetheless, materials are not the unique tendency regarding the optimization of thermoelectric modules. It is also important to consider the geometrical configuration of the thermocouples: length, number of elements, cross-sectional area or the combination of materials within a thermocouple (the so-called segmented thermoelectric modules) among others [10–17].

Besides the improvement of thermoelectric modules, other aspects of a thermoelectric generator can be optimized in order to improve net generation. As shown in **Figure 1**, a thermoelectric generator is formed by one or multiple modules interconnected that generate electricity based on the heat received from a hot source, and emit the rest to a cold sink, which is normally the environment. Since the efficiency of the system increases as the sides of the thermoelectric modules approach the temperature of the heat source and sink, the introduction of heat exchangers between the modules and each of the thermal reservoirs becomes necessary in order to maximize the temperature difference.

In this sense, it is widely known that the optimization of heat exchangers is of utmost importance [9, 18–24]. Obtaining low thermal resistances maximizes the temperature difference, and consequently increases the efficiency of the entire generator. In fact, for a particular geometry it was demonstrated that a 10% improvement of the thermal resistance causes an increase of 8% in the electric power generation [25].

http://dx.doi.org/10.5772/intechopen.75697

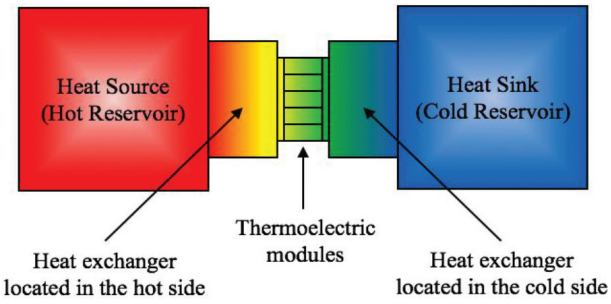

Figure 1. Basic diagram of a thermoelectric generator.

However, optimization processes often forget the assembly of the generator, i.e. how the different parts are interconnected. And this is something to definitely take into account since a poor assembly can waste the performance of the whole generator regardless having optimal modules and heat exchangers. Thus, the present chapter analyzes three different aspects that need to be considered in the assembly of a thermoelectric generator.

Section 2 deals with the interface contact, or how the microscopic unevenness can affect heat transfer. Section 3 shows the importance of having a uniform pressure distribution in order to ensure a good contact between the different parts. Section 4 explains how to reduce the thermal bridges, undesirable heat losses. Finally, Section 5 summarizes and concludes the chapter.

2. Interface contact

When two surfaces are confronted, it may seem that there exists a perfect contact among them. However, due to their roughness, surfaces are only in touch at some points, being mostly separated by air gaps that reduce the heat transmission in the interface (**Figure 2**). In thermoelectric generators, this fact attenuates the temperature difference across the thermoelectric modules, and therefore, decreases the output power. Thus, the present section explains how to quantify and improve the contact between the modules and each heat exchanger that compose a thermoelectric generator.

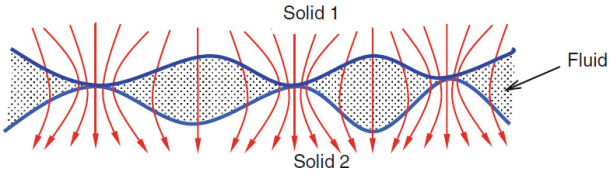

Figure 2. Representation of the interface filled with air. Red lines simulate the heat flux through the interface [26].

2.1. Thermal interface materials

In order to improve the contact and achieve a low temperature drop, thermal interface materials (TIMs) are used [27]. Their purpose consists in filling the gaps with materials that have a higher thermal conductivity than air. There are many families of thermal interface materials such as graphite sheets, thermal greases, phase change materials, indium or elastomers [28–30]. With the objective of checking if the presence of TIMs improves the real contact, this section analyzes three of the most common interface configurations for thermoelectric generators: without TIM, with graphite sheets, and with silicone thermal grease. The specific characteristics of these TIMs are described in **Table 1**.

The effect of the thermal contact is modeled through the thermal contact resistance (Eq. (2)), which depends on the temperature drop across the interface ΔT, the heat flux $\dot{Q}$ and the area A. This parameter takes into consideration that, due to imperfections in the material's surface, the real contact area is just a small fraction of the apparent contact area; and it is defined in such a way that it is also independent of the TIM's thickness, which varies with pressure.

$$R_{co} = \frac{\Delta T \cdot A}{\dot{Q}} \tag{2}$$

This thermal resistance depends on many parameters: materials of the contact (with their respective roughness, hardness, and conductivity), their geometry, interface temperature, or contact pressure among others. Therefore, it is difficult to obtain a general expression valid for all assembly possibilities and that considers all the variables. All the expressions available in the literature are restricted to particular geometries and only take into account some of the depending parameters [31–33]. In this sense, the present section focuses on obtaining the thermal contact resistance for the standard dimensions of a thermoelectric module (40×40 mm^2) depending on the clamping pressure and considering a side temperature of 100°C.

2.2. Methodology

Due to the broad parameter dependence of the thermal contact resistance, the test bench of **Figure 3b** has been used in order to measure thermal contact resistances for thermoelectric modules' dimensions in a controlled environment. This device is based on the principle of 'steady state' measurements across thermal interface material junctions.

Hence, a known heat is forced to flow through two 40×40 mm^2 reference bars (usually called fluxmeters) separated by the TIM of interest and under a certain pressure. Thanks to

	Thermal conductivity (W/m·K)	Operation temperature (°C)	Thickness (mm)
Graphite sheet	10	−40 to 400	0.127
Polydimethylsiloxane oil-based silicone thermal grease	0.41	−40 to 250	—

Table 1. Properties of thermal Interface materials.

http://dx.doi.org/10.5772/intechopen.75697

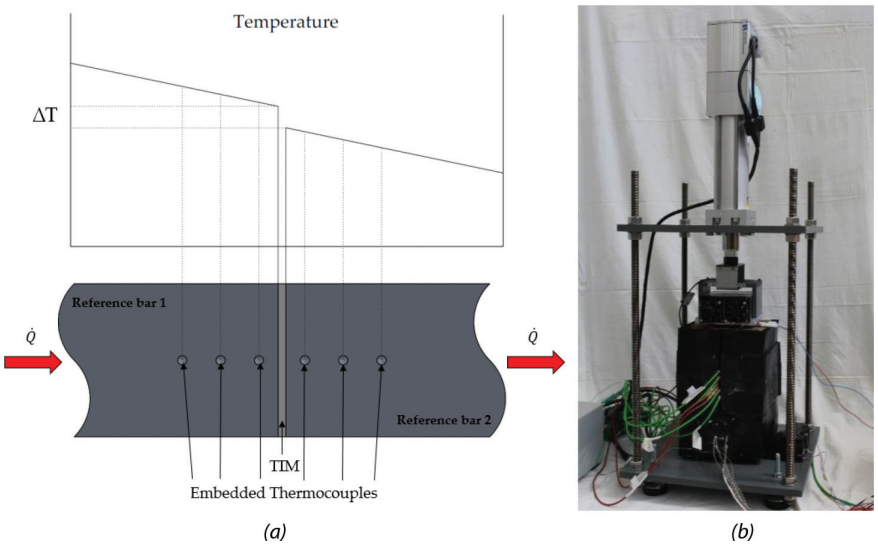

Figure 3. (a) Extrapolation method and (b) thermal contact resistance test bench for thermoelectric generation applications.

thermocouples embedded in these bars and since their conductivities are perfectly known, the temperature drop across the interface (ΔT) can be indirectly calculated by extrapolation (**Figure 3a**). Thermal contact resistance is therefore calculated with Eq. (2). Heat flux across the interface of Eq. (2) is generated by an electrical resistance and dissipated by a heat sink with a fan. Its calculation is possible thanks to the reference bars conductivity, thermocouples measurements and their distance.

Two dissimilar materials of the reference bars were used to test TIMs: highly conductive but soft 1050 Aluminum alloy and a cupper-tungsten alloy which presents an excellent relation between thermal conductivity and hardness. The specific properties (thermal conductivity, hardness, and roughness) of each of these materials are described in **Table 2**.

For each material, the three mentioned possible interfaces were studied: no TIM, graphite sheets and silicone thermal grease. All the experiments were performed under the same conditions. The only variable was pressure, one of the most influent parameters in thermal interface resistances, and which was exerted by a linear actuator. The studied pressures range between 50 and 1200 kPa because the pressure recommended by the thermoelectric modules manufacturer is around 1000 kPa [34].

Material	Thermal conductivity (W/m·K)	Hardness (HB)	Ra (μm)	Rz (μm)
Al 1050	229	21	0.090	1.275
W75Cu25	170	200	0.126	1.215

Table 2. Materials and properties of the fluxmeter bars.

In contact resistance measurement with the 'steady state method,' uncertainty calculation must be taken into account due to the large number of measures that are made. The uncertainty calculation method used is the same as other authors in the literature [35–38] when applying the same method to measure thermal contact resistances. **Table 3** shows the uncertainty values of the equipment.

2.3. Results and discussion

Firstly, results of the interface thermal resistance using aluminum bars are shown in **Figure 4a**. For all the studied interfaces, the behavior with respect pressure follows a similar trend: the thermal resistance decreases with pressure. Hence, the worst value is obtained at low pressures. In addition, it is confirmed that is better to use TIM instead of not using it; the highest thermal resistance corresponds to the absence of TIM. The thermal grease improves the contact without TIM, but when the pressure is higher, its presence is negligible. The reason is that the grease pumps out of the interface at high pressures. Therefore, thermal grease would not improve the contact in assemblies at elevated pressures. Graphite sheets seem to be better: thermal contact resistance is enhanced at every pressure point. The smallest value of thermal resistance obtained for graphite sheet is 2.19×10^{-5} K·m^2/W for the Aluminum interface at 1183 kPa.

Secondly, results of cupper-tungsten alloy bars are shown in **Figure 4b**. These bars have a higher hardness, and its influence can be observed in the results. Due to its higher hardness, thermal resistance without TIM is again the worst one and almost three times higher than with aluminum. In contrast, graphite sheet shows different results than before: its thermal resistance at low pressures is higher than thermal grease. Nevertheless, if the pressure increases, the behavior of the graphite sheets improves, being better than the thermal grease. Thus, on very hard surfaces thermal grease is very effective at low pressures due to its fluidity, and graphite sheet needs higher pressures to work well.

Hence, it can be said that thermal contact resistance must definitely be considered in thermoelectric assemblies because it produces a temperature drop across the interfaces that decreases the efficiency of thermoelectric generators. In order to reduce these thermal contact resistances, the use of thermal interface materials has been demonstrated regardless the

Measured parameter (x_i)	U_i
Temperature (thermocouple)	± 0.3 K
Temperature sensor location	± 300 μm
Force	± 0.2%
Hole distance	± 10 μm
Thermal conductivity	± 10%

Table 3. Uncertainties table.

pressure. Among the studied TIMs, graphite is better for most of the cases. Nonetheless, hardness seems to be an important parameter to consider, with graphite being the most affected by this at low pressures. Thus, on very hard surfaces working with at low pressures, thermal grease presents a better behavior, reducing the temperature drop.

3. Influence of pressure distribution

Last section has shown the importance of achieving a low thermal contact resistance in the assembly of thermoelectric generators since it can affect the performance of the whole system. However, this is not always an easy task, and the introduction of thermal interface materials becomes necessary to ensure a good contact at microscopic level. Furthermore, the combination of pressure with these thermal interface materials improves even further the contact between surfaces as shown in **Figure 4**. These graphs analyze different thermal interface materials and different uniform pressure distributions. But what happens if the pressure distribution is not uniform?

Pressure distribution basically depends on the assembly, i.e. the location and the torque applied to the screws. Hence, if there is an uneven torque in the screws or if the location is not appropriate or even if the exerted torque is too big that it provokes the bending of the heat exchangers, it could happen that only some parts of the thermoelectric modules are in contact with the heat exchangers, leading to changes associated with the thermal contact resistance explained in last section [39, 40]. As a consequence, temperature mismatches appear and therefore problems of decreased power output arise [41]. Thus, although it is not normally taken into account, it is important to consider the clamping force in the assembly of thermoelectric generators [42, 43]. In this sense, the present section analyzes different screw configurations and torques to demonstrate the importance of the clamping pressure and its distribution in the assembly of thermoelectric generators.

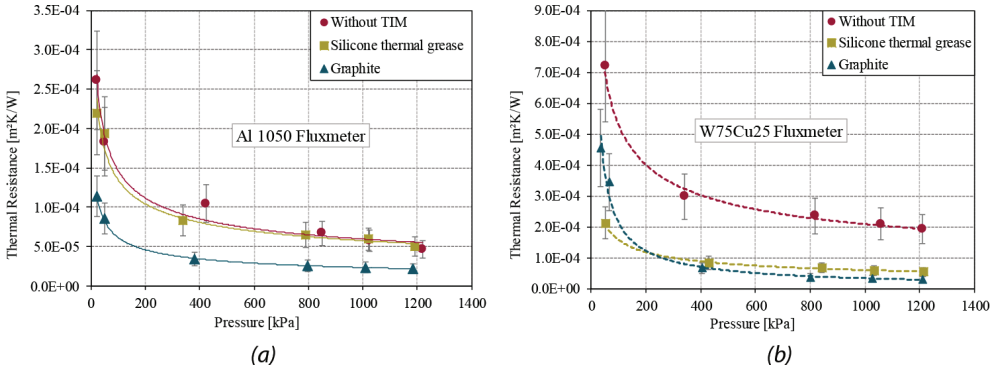

Figure 4. (a) Thermal resistance of TIMs in an aluminum interface at 100°C and (b) thermal resistance of TIMs in a copper-tungsten alloy interface at 100°C.

3.1. Methodology

3.1.1. Description of the studied configurations

In order to analyze how the pressure is distributed with regard the location of the screws and their torque, two different thermoelectric generators have been used with graphite as interface material since it has been demonstrated that it leads to better results than the other studied TIMs. In both generators, the heat source is represented by a heating plate made up of electrical resistances, in contact with the thermoelectric modules, which dissipate the non-converted heat to the ambient thanks to a fin dissipater assisted by a ventilator. The dimensions are the only difference between them. Hence, one of the generators is prepared for holding two thermoelectric modules while the bigger dimensions of the second one allows the implementation of four modules. For each generator, two possible screw configurations clamped with different torques have been analyzed. The location of the screws is depicted in **Figure 5**, while the studied torques are summarized in **Table 4**.

3.1.2. Study of the pressure distribution

Pressure distribution has been studied thanks to PRESCALE Pressure Measurement Films by Fujifilm [44]. These films change their color intensity depending on the pressure applied, changing from white to dark magenta as pressure increases. In this particular case, films ranged between 0.6 and 2.5 MPa have been used.

For each of the experiments, a film has been placed between the thermoelectric modules and the fin dissipater located at the cold side. With this film suitably located, the generator has been assembled with the corresponding torques. As a consequence, the films changed their color in those areas where more pressure was exerted. After the generator was perfectly assembled, the set was cautiously dismantled and the films analyzed. Experiments were repeated three times each in order to ensure their repetitiveness.

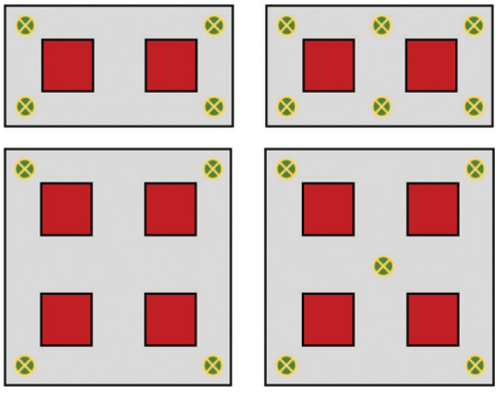

Figure 5. The four studied screw configurations for the considered thermoelectric generators.

Number of modules	Number of screws	Torque (Nm)
2	4	1
	6	1
	6	1.5
	6	2
4	4	1
	5	2

Table 4. Summary of the studied torques for the different configurations.

The analysis has been performed in two steps. On the one hand, a qualitative analysis has allowed the visual determination of the pressure distribution. On the other hand, the comparison of each of the pixels with a scale by means of the closest neighbor method has permitted a statistical analysis, with the median as the most important parameter.

3.2. Results and discussion

3.2.1. Qualitative analysis

Based on the pressure films, it is obvious that there does not exist a uniform pressure distribution in the modules. **Figure 6a** shows the distribution obtained in the configuration with two modules and four screws. As it can be observed, only those parts closer to the screws have a significant pressure. The central part of the configuration seems not to be in such a good contact due to the bending of the base of the dissipator.

If another two screws are introduced in order to reduce the mentioned bending (**Figure 6b–d**), the pressure distribution becomes more uniform. The reason why the distribution is not equally uniform at both sides of the modules is due to the different distance of the screws to the modules. Nonetheless, as expected, it is achieved a higher intensity of this pressure as the torque increases.

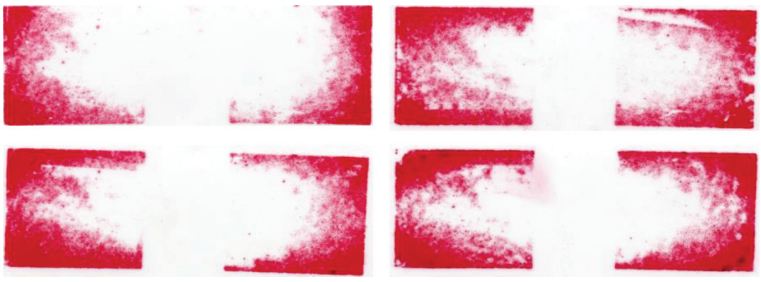

Figure 6. Pressure films for (a) 4 screws, 1 Nm; (b) 6 screws, 1 Nm; (c) 6 screws, 1.5 Nm; and (d) 6 screws, 2 Nm.

In the case of having four modules in an assembly with only four screws, the fact that pressure is not uniformly distributed becomes more noticeable. Only the four corners, where screws are actually located, are working under an appreciable pressure (**Figure 7a**).

If an additional screw is located in the center so that the bending of the dissipater is reduced and the pressure is increased in order to improve the contact, the improvements obtained are minimal (**Figure 7b**) due to the big distance between the additional screw and the modules. Thus, it is recommended that each module has its own tightening.

3.2.2. Quantitative analysis

Visual analysis of **Figures 6** and **7** states a pressure distribution which is far from uniformity. In this section, this fact is demonstrated with a statistical analysis based on the median. Since the pressure films used for the experiments are ranged from 0.6 to 2.5 MPa, those parts that work with a pressure out of scale will not be appropriately represented. Thus, the median is the most significant parameter to analyze: half of the pixels work under that pressure while the other half works above it.

On the one hand, for the heat exchanger with two modules, in the case in which there are only four screws, most of the module works under a pressure of 0.6 MPa or less. This value improves if the bending is restricted by means of an additional pair of screws located between the modules. As shown in **Figure 8**, and accordingly to the previous states, the median of the pressure increases with the torque in a proportion that seems linear.

On the other hand, in the heat exchanger with four modules, the lack of macroscopic contact is evident with the median value of 0.6 MPa, i.e. most parts of the modules have a clamping pressure of less than 0.6 MPa. Nonetheless, although the visual analysis evinces a slight improvement when the fifth screw is introduced and a more significant torque exerted, this fact is not appreciable in the median value since the range of pressures of both configurations is much lower than 0.6 MPa, the lower limit of the scale of the film.

Hence, despite not being considered a critical aspect, screw distribution and torque are aspects to definitely take into account. The assembly configuration determines the pressure

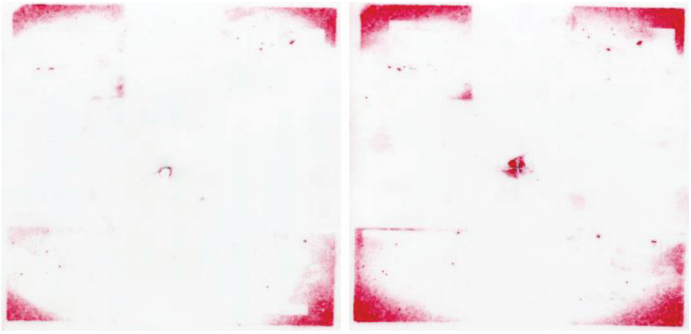

Figure 7. Pressure films for (a) four screws, 1 Nm (b) five screws, 2 Nm.

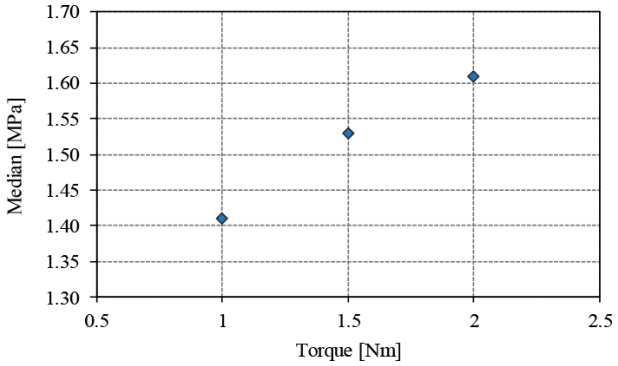

Figure 8. Median of the pressure against the applied torque for the configuration of two modules.

distribution in the modules, which is in turn related to the thermal contact resistance. If the module works under an uneven pressure distribution, the generation will be reduced, since some parts of the module can even be not in contact with the heat exchangers.

The most appropriate configuration seems that in which each module has the biggest amount of screws as close as possible to it. Furthermore, as the torque of these screws increases, the clamping pressure will get bigger as well as better distributed, and therefore, the thermal contact resistance will be reduced, leading to a better generation unless bending is provoked.

4. How to avoid thermal bridges

Last section has concluded that it is recommended to have an individual tightening of the modules in order to ensure a uniform pressure distribution that leads to a good thermal contact. In order to achieve it, screws are necessary although they represent a type of thermal bridge.

By definition, a thermal bridge is an area or component of an object which has higher thermal conductivity than the surrounding materials, creating a path of least resistance for heat transfer [45, 46]. In thermoelectric generators, there are two main sources for thermal bridges. On the one hand, the screws used to ensure a good contact and pressure distribution are normally metallic, and therefore, highly thermal conductive. In order to reduce the amount of heat lost through these screws, it is typical to use nylon washers. Nonetheless, even with this nylon rings, it is estimated that the thermal resistance of each screw is 52 K/W.

On the other hand, due to the small thickness of the thermoelectric modules (most commonly 3 mm), it can occur that part of the heat directly flows within the heat exchangers, instead of through the thermoelectric modules. Therefore, insulating materials are usually inserted between the heat exchangers.

In the present section, assuming there is a good thermal contact, three different alternatives of insulating materials that are normally used in order to avoid thermal bridges will be studied:

- Mineral wool fiber cardboard manufactured by Nefalit. This material is made up of highly thermal insulating fibers bound together with fillers. These plates are suitable for temperatures up to 750 or 1000°C and are easy to handle in the assembly. They present a thermal conductivity of 0.15 W/mK [47].
- Acrylic wool made by Flexiband: this insulating material is manufactured from pure refractory fibers which provide a low thermal conductivity (0.09 W/mK) and flexibility [48].
- Air: known as one of the best insulators, air presents a thermal conductivity of 0.024 W/mK. Nevertheless, if convection currents are created, heat transfer coefficients improve and the effective value of the thermal conductivity can be considerably increased.

4.1. Methodology

For each of these insulating materials, the assembly depicted in **Figure 9** was mounted. A heating plate acts as a heat source, providing a power, $\dot{Q}_{source}$, of 100, 150 or 200 W. This plate is in direct contact with two thermoelectric modules surrounded by the insulating material of study in each case. In the cold side of the thermoelectric modules, there is a fin dissipater assisted by a ventilator. In order to minimize direct thermal losses from the heating plate to the environment, a 50 mm layer of rock wool has been used.

Figure 9 also shows the location of the type K thermocouples installed. Hence, the three involved heat fluxes can be determined: the heat flux that goes through the modules and therefore is responsible of the electric generation, $\dot{Q}_{\mathrm{mod}}$; the heat flux lost due to the thermal bridges, $\dot{Q}_{tb}$; and the heat flux that is directly lost from the source to the ambient, $\dot{Q}_{amb}$. This last heat flux has been calculated thanks to the insulation and the ambient temperatures in conjunction with a convection coefficient of $h = 5$ W/m^2 K [49].

$$\dot{Q}_{amb} = h \cdot A \cdot \left(T_{ins} - T_{amb}\right) \tag{3}$$

In contrast, the calculation of the other two heat fluxes has required the use of a computational model. Temperatures T_c and T_h are known, but thermal resistances depend on the thermal contacts between the different parts, $R_{co,h}$ and $R_{co,c}$, as well as on the existing temperature distribution in each case. Thus, the computational model based on the finite difference method of **Figure 10** has been used. This model calculates all the possible thermal resistances of the modules, R_{mod}, and their generating voltage depending on the temperature difference and the load resistance, with an error less than 10% [50]. By comparing the experimental temperature difference and the open circuit voltage determined by the model, both the thermal contact resistances and the thermoelectric modules resistance have been estimated.

Based on them, the different heat fluxes can be computed as follows. Firstly, the heat that is supposed to flow through the modules is the heat provided by the source minus the heat directly lost to the environment.

$$\dot{Q}_h = \dot{Q}_{source} - \dot{Q}_{amb} \tag{4}$$

http://dx.doi.org/10.5772/intechopen.75697

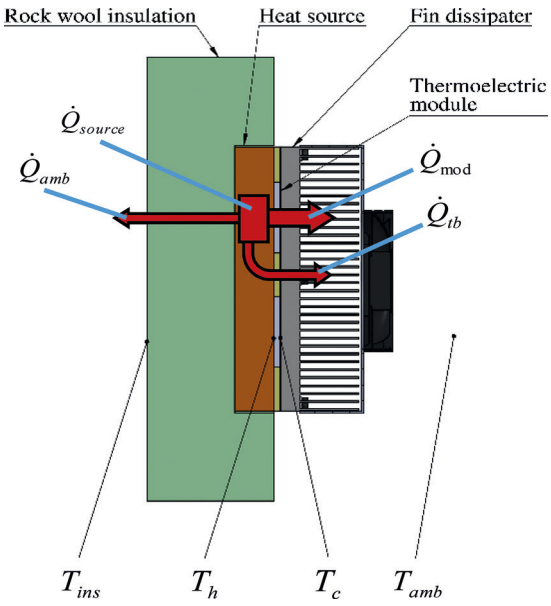

Figure 9. Schematic view of the studied configuration with specification of the position of the type K thermocouples installed and the heat fluxes considered.

Secondly, the heat that goes through the modules is computed with the mentioned thermal resistances, the measured temperature difference and the number of modules *M*.

$$\dot{Q}_{\text{mod}} = \frac{M \cdot (T_h - T_c)}{R_{co,h} + R_{\text{mod}} + R_{co,c}} \tag{5}$$

Finally, the heat that is lost in the thermal bridge can be computed as the difference between the heat that is supposed to flow through the modules, and the heat that actually passes through them.

$$\dot{Q}_{tb} = \dot{Q}_h - \dot{Q}_{\text{mod}} \tag{6}$$

Nonetheless, the percentage values of the heat that goes through the thermal bridges instead of the modules acquires more interest:

$$\%\dot{Q}_{tb} = \frac{\dot{Q}_{tb}}{\dot{Q}_h} \cdot 100 \tag{7}$$

The repetitiveness of the experiments has been ensured by means of mounting and dismounting the ensemble three times for each configuration, which also reduces the uncertainty of the measurements and the experimental procedure.

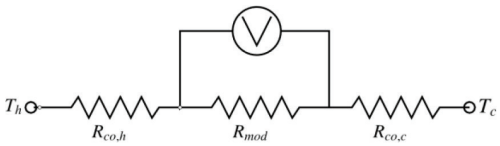

Figure 10. Thermal-electric analogy of the computational model.

4.2. Results and discussion

In a first approach, **Figure 11** shows the results obtained for the configuration in which the insulating material has the same thickness as the module, i.e. 3 mm (**Figure 12**). As it can be observed, for all the studied materials, the percentage of heat lost through the insulation increases with the heat dissipated by the source. Nonetheless, this amount differs for each material. Thus, cardboard presents the most significant heat losses, with almost 30% lost due to thermal bridges. This is the expected result since it presents the highest conductivity of the studied materials. However, despite the air having the smallest thermal resistance, the thickness between both heat exchangers is enough to create convection currents that improve the heat transfer. As a result, thermal losses with either acrylic wool or air as insulators are similar. Furthermore, it is worth mentioning that in the case of having air, which is equivalent to not putting anything, the assembly is more complicated since modules can easily move, as they are not held by the insulating material.

Since thermal losses represent a considerable part of the heat that should go through the modules, a second configuration (**Figure 13**) with a higher distance between the heat exchangers increases was also studied. Increasing the thickness of the insulation causes an increment of the thermal resistance, and therefore, thermal losses should decrease. This increment of thickness

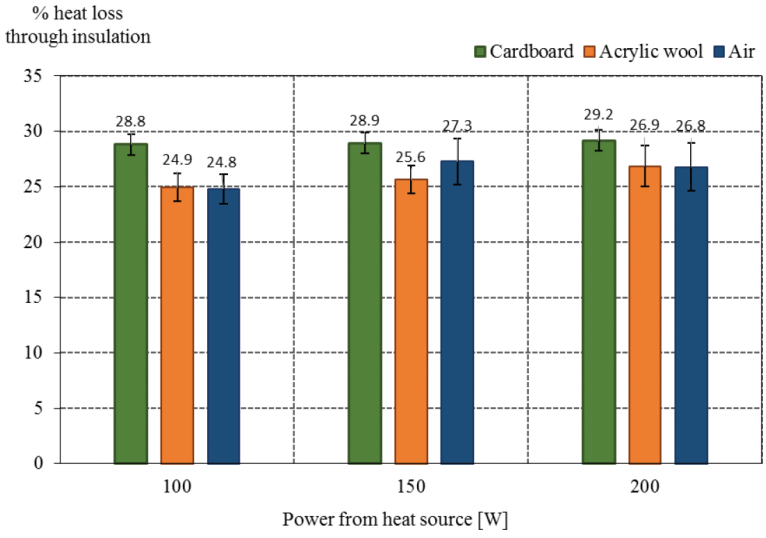

Figure 11. Percentage of heat loss through insulation for different heat powers in absence of heat extenders.

http://dx.doi.org/10.5772/intechopen.75697

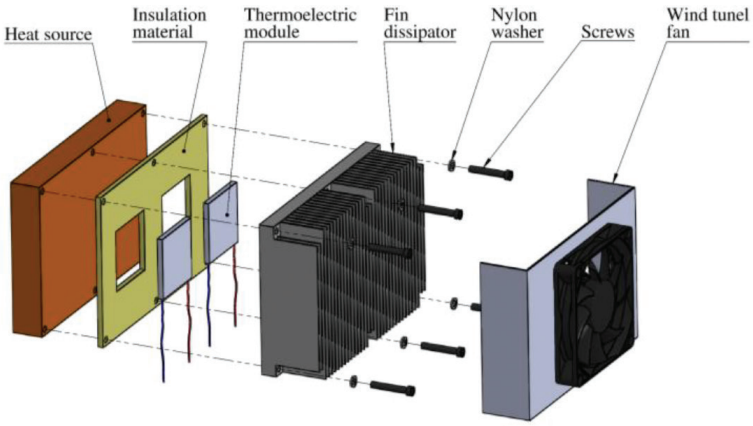

Figure 12. Exploded view of the studied generator without heat extenders.

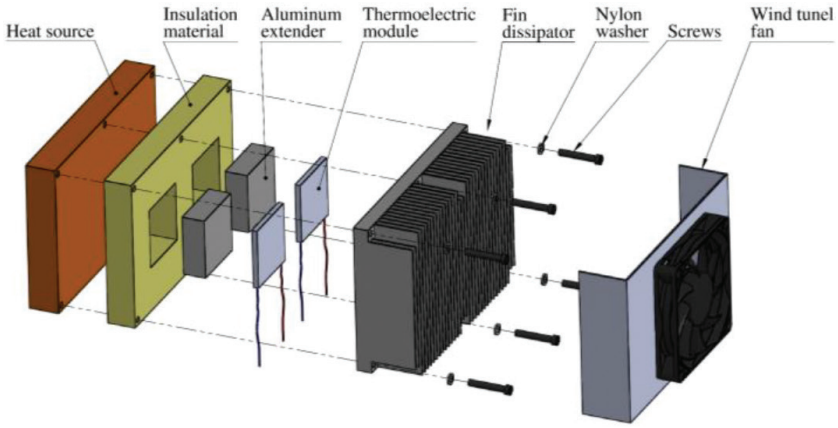

Figure 13. Exploded view of the studied generator with heat extenders.

is compensated with highly conductive aluminum heat extenders in the case of the modules. Nonetheless, this leads to two additional contacts, with their associated thermal contact resistance, which can negatively influence the thermal transfer if contact is not appropriated. In this case, graphite sheets have again been used as TIM in order to ensure the microscopic contact.

As it can be observed in **Figure 14**, the increment of distance between the heat exchangers supposes a reduction of approximately 5% in the percentage of heat that is lost due to thermal bridges since, as expected, thermal resistances of the insulation increase leading to less thermal losses. For this configuration, the tendency remains similar: heat losses increase with the power from the heat source and acrylic wool is still the best insulator and cardboard the worst. However, differences between acrylic wool and air are now more evident. Since the distance between the exchangers has increased, there is more space for the convection currents to flow, this improving the heat transfer and leading to more thermal losses.

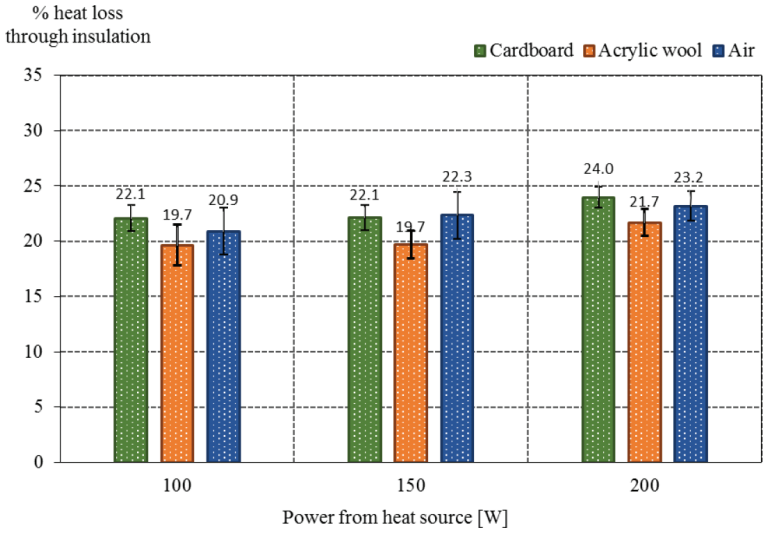

Figure 14. Percentage of heat loss through insulation for different heat powers in the case of introducing heat extenders.

In summary, losses due to thermal bridges definitely need to be taken into account: around one-fourth of the power provided from the source goes through the insulation instead of the thermoelectric modules. As a consequence, the generation is reduced.

In order to decrease the thermal losses, it has been demonstrated that it is better to increase the thickness of the insulation, despite adding two additional contacts. Among the materials studied, the best one is acrylic wool. Nonetheless, air (equivalent to not adding any insulation) should be considered, since the cost is reduced and there is not such a significant difference among them. However, it presents the disadvantage of a more complicated assembly.

5. Conclusions

Although the assembly is not generally considered in the optimization of thermoelectric generators, the present chapter has demonstrated that it is an aspect that cannot be forgotten since it deteriorates the performance of generators. Thus, the assembly needs to incorporate thermal interface materials that counteract microscopic imperfections, being graphite sheets the most recommended one between the studied. In order to ensure this microscopic contact and reduce the temperature drop that appears in the interface, it is also important to apply some pressure to the assembly. The easiest way to achieve this is the use of screws. Pressure measurement films have shown that each module needs to have its own tightening. Assemblies that share this tightening can cause a contact in only some parts of the module. However, the implementation of these screws has a counter effect: they represent a thermal bridge themselves and part of the heat is lost through them. Therefore, the insertion of nylon rings is recommended. The other important source of losses due to thermal bridges occurs between the heat exchangers, since the distance between them is too small. Placing an insulating material between the exchangers slightly reduces the losses, but it is better to

increase the distance between them with the aid of a conductive heat extender and insulate with acrylic wool. Nonetheless, if this material is not added, air has demonstrated to also be a good insulator, cheaper but which leads to a less precise assembly.

Acknowledgements

The authors are indebted to the Ministry of Economy, Industry and Competitiveness-Government of Spain and FEDER Funds for economic support of this work, included in the DPI2014-53158-R Research Project, as well as to the FPU Program of the Spanish Ministry of Education, Culture and Sport (FPU16/05203).

Nomenclature

α	Seebeck coefficient, V/K
λ	thermal conductivity, W/mK
ρ	electrical resistivity, Ωm
A	contact area, m^2
h	free convection coefficient, W/m^2K
M	number of thermoelectric modules
n	relative to type-n semiconductor
p	relative to type-p semiconductor
$\dot{Q}$	heat flux through the interface, W
$\dot{Q}_{amb}$	heat flux losses to ambient through insulation, W
$\dot{Q}_h$	heat through thermoelectric generator, W
$\dot{Q}_{\mathrm{mod}}$	heat through thermoelectric modules, W
$\dot{Q}_{source}$	heat provided by heating plate, W
$\dot{Q}_{tb}$	heat flux due to thermal bridges, W
R_a	arithmetical mean roughness (μm)
R_z	ten-point mean roughness (μm)
R_{co}	thermal contact resistance, Km^2/W
$R_{co,h}$; $R_{co,c}$	contact thermal resistance of hot and cold side, K/W
R_{mod}	thermal resistance of the modules, K/W
T_{amb}	ambient temperature, K
T_c	module cold face temperature, K

T_h	module hot face temperature, K
T_{ins}	insulation temperature, K
U_i	uncertainty in the measurement x_i
x_i	each measurement made in experiments
Z	figure of merit
ΔT	temperature drop across interface, K

Author details

Miguel Araiz[1,2]*, Leyre Catalan[1,2], Oscar Herrero[1], Gurutze Perez[1,2] and Antonio Rodriguez[1,2]

*Address all correspondence to: miguel.araiz@unavarra.es

1 Public University of Navarre, Pamplona, Spain

2 Institute of Smart Cities, Pamplona, Spain

References

[1] Abelson RD. Space Missions and Applications. Thermoelectr. Handb. Macro to nano2. 1st ed. Boca Raton: CRC Press; 2006, pp. 56.1-56.29

[2] Rowe D. General Principles and Considerations. Thermoelectr. Handb. Macro to Nano. Boca Raton: CRC Press; 2006. pp. 1.1-1.14

[3] Romanjek K, Vesin S, Aixala L, Baffie T, Bernard-Granger G, Dufourcq J. High-performance silicon–germanium-based thermoelectric modules for gas exhaust energy scavenging. Journal of Electronic Materials. 2015;**44**:2192-2202. DOI: 10.1007/s11664-015-3761-1

[4] Lee S, Lee KH, Kim YM, Kim HS, Snyder GJ, Baik S, et al. Simple and efficient synthesis of nanograin structured single phase filled skutterudite for high thermoelectric performance. Acta Materialia. 2018;**142**:8-17. DOI: 10.1016/j.actamat.2017.09.044

[5] Aswal DK, Basu R, Singh A. Key issues in development of thermoelectric power generators: High figure-of-merit materials and their highly conducting interfaces with metallic interconnects. Energy Conversion and Management. 2016;**114**:50-67. DOI: 10.1016/j.enconman.2016.01.065

[6] Gayner C, Kar KK. Recent advances in thermoelectric materials. Progress in Materials Science. 2016;**83**:330-382. DOI: 10.1016/j.pmatsci.2016.07.002

[7] Twaha S, Zhu J, Yan Y, Li B. A comprehensive review of thermoelectric technology: Materials, applications, modelling and performance improvement. Renewable and Sustainable Energy Reviews. 2016;**65**:698-726. DOI: 10.1016/j.rser.2016.07.034

[8] Champier D. Thermoelectric generators: A review of applications. Energy Conversion and Management. 2017;**140**:167-181. DOI: 10.1016/j.enconman.2017.02.070

[9] Elghool A, Basrawi F, Ibrahim TK, Habib K, Ibrahim H, Idris DMND. A review on heat sink for thermo-electric power generation: Classifications and parameters affecting performance. Energy Conversion and Management. 2017;**134**:260-277. DOI: 10.1016/j.enconman.2016.12.046

[10] Min G. Thermoelectric Modules Design Theories. Thermoelectr. Handb. Macro to Nano. 1st ed. Boca Raton: CRC Press; 2006. pp. 11.1-11.15

[11] Rowe DM, Min G. Optimisation of thermoelectric module geometry for waste heat electric power generation. Journal of Power Sources. 1992;**38**:253-259

[12] Vián JG, Astrain D, Rodríguez A, Martínez A. Computational optimization of a thermoelectric ice-maker as a function of the geometric parameters of a peltier module. Journal of Electronic Materials. 2010;**39**:1786-1791. DOI: 10.1007/s11664-010-1134-3

[13] Chen W-H, Wu P-H, Lin Y-L. Performance optimization of thermoelectric generators designed by multi-objective genetic algorithm. Applied Energy. 2018;**209**:211-223. DOI: 10.1016/j.apenergy.2017.10.094

[14] Ma Q, Fang H, Zhang M. Theoretical analysis and design optimization of thermoelectric generator. Applied Thermal Engineering. 2017;**127**:758-764. DOI: 10.1016/j.applthermaleng.2017.08.056

[15] Kishore RA, Sanghadasa M, Priya S. Optimization of segmented thermoelectric generator using Taguchi and ANOVA techniques. Scientific Reports. 2017;**7**:16746. DOI: 10.1038/s41598-017-16372-8

[16] Brownell E, Hodes M. Optimal design of thermoelectric generators embedded in a thermal resistance network. IEEE Transactions on Components, Packaging, and Manufacturing Technology. 2014;**4**:612-621. DOI: 10.1109/TCPMT.2013.2295169

[17] Aranguren P, Roch A, Stepien L, Abt M, Von Lukowicz M, Dani I, et al. Optimized design for flexible polymer thermoelectric generators. Applied Thermal Engineering. 2016;**102**:402-411. DOI: 10.1016/j.applthermaleng.2016.03.037

[18] Astrain D, Martínez Á. Heat exchangers for thermoelectric devices. Heat exchangers - Basics Design Applications. 2012:289-308. DOI: 10.5772/33464

[19] Aranguren P, Astrain D, Rodriguez A, Martinez A. Net thermoelectric power generation improvement through heat transfer optimization. Applied Thermal Engineering. 2017;**120**:496-505. DOI: 10.1016/j.applthermaleng.2017.04.022

[20] Dent Jr TJ, Agrawal AK. Role of thermal strategies in thermoelectric power generation. 50th AIAA Aerosp. Sci. Meet. Incl. New Horizons Forum Aerosp. Expo; 2012. pp. 2012-520

[21] Su CQ, Wang WS, Liu X, Deng YD. Simulation and experimental study on thermal optimization of the heat exchanger for automotive exhaust based thermoelectric generators. Case Studies in Thermal Engineering. 2014;**4**:85-91

[22] Zhou S, Sammakia BG, White B, Borgesen P, Chen C. Multiscale modeling of thermoelectric generators for conversion performance enhancement. International Journal of Heat and Mass Transfer. 2015;**81**:639-645

[23] Martínez A, Vián JG, Astrain D, Rodríguez A, Berrio I. Optimization of the heat exchangers of a thermoelectric generation system. Journal of Electronic Materials. 2010;**39**:1463-1468. DOI: 10.1007/s11664-010-1291-4

[24] Lv S, He W, Jiang Q, Hu Z, Liu X, Chen H, et al. Study of different heat exchange technologies influence on the performance of thermoelectric generators. Energy Conversion and Management. 2018;**156**:167-177. DOI: 10.1016/j.enconman.2017.11.011

[25] Astrain D, Vián JG, Martínez A, Rodríguez A. Study of the influence of heat exchangers' thermal resistances on a thermoelectric generation system. Energy. 2010;**35**:602-610. DOI: 10.1016/j.energy.2009.10.031

[26] Madhusudana CV. Thermal Contact Conductance. In: Ling FF editor. Switzerland: Springer International Publishing; 2014. DOI: 10.1007/978-3-319-01276-6. ISBN: 978-319-01275-9

[27] Sakamoto T, Iida T, Sekiguchi T, Taguchi Y, Hirayama N, Nishio K, et al. Selection and evaluation of thermal interface materials for reduction of the thermal contact resistance of thermoelectric generators. Journal of Electronic Materials. 2014;**43**:3792-3800. DOI: 10.1007/s11664-014-3165-7

[28] Prasher R. Thermal interface materials: Historical perspective, status, and future directions. Proceedings of the IEEE. 2006;**94**:1571-1586. DOI: 10.1109/JPROC.2006.879796

[29] Gwinn JP, Webb RL. Performance and testing of thermal interface materials. Microelectronics Journal. 2003;**34**:215-222. DOI: 10.1016/S0026-2692(02)00191-X

[30] Due J, Robinson AJ. Reliability of thermal interface materials: A review. Applied Thermal Engineering. 2013;**50**:455-463. DOI: 10.1016/j.applthermaleng.2012.06.013

[31] Fletcher LS. Prediction of Thermal Contact Conductance between Similar Metal Surfaces. Heat Transf. Spacecr. Therm. Control, New York: American Institute of Aeronautics and Astronautics; 1971. pp. 273-88. DOI: 10.2514/5.9781600864988.0273.0288

[32] Mikić BB. Thermal contact conductance; theoretical considerations. International Journal of Heat and Mass Transfer. 1974;**17**:205-214. DOI: 10.1016/0017-9310(74)90082-9

[33] Cooper MG, Mikic BB, Yovanovich MM. Thermal contact conductance. International Journal of Heat and Mass Transfer. 1969;**12**:2. DOI: 10.1016/0017-9310(69)90011-8

[34] Marlow Industries. Technical Data Sheet: Tg12-8-01Ls Power Generators n.d.:1-2

[35] Kempers R, Kolodner P, Lyons A, Robinson AJ. A high-precision apparatus for the characterization of thermal interface materials. The Review of Scientific Instruments. 2009;**80**:95111. DOI: 10.1063/1.3193715

[36] Smith AN, Jankowski NR, Boteler LM. Measurement of high-performance thermal interfaces using a reduced scale steady-state tester and infrared microscopy. Journal of Heat Transfer. 2016;**138**:41301. DOI: 10.1115/1.4032172

[37] Hao M, Saviers KR, Fisher TS. Design and validation of a high-temperature thermal Interface resistance measurement system. Journal of Thermal Science and Engineering Applications. 2016;**8**:31008. DOI: 10.1115/1.4033011

[38] Warzoha RJ, Smith AN, Harris M. Maximum resolution of a probe-based, steady-state thermal interface material characterization instrument. Journal of Electronic Packaging. 2016;**139**:11004. DOI: 10.1115/1.4035178

[39] Montecucco A, Buckle J, Siviter J, Knox AR. A new test rig for accurate nonparametric measurement and characterization of thermoelectric generators. Journal of Electronic Materials. 2013;**42**:1966-1973. DOI: 10.1007/s11664-013-2484-4

[40] Yeh C, Wen C, Chen Y, Yeh S, Wu C. An experimental investigation of thermal contact conductance across bolted joints. Experimental Thermal and Fluid Science. 2001;**25**:349-357. DOI: 10.1016/S0894-1777(01)00096-6

[41] Montecucco A, Siviter J, Knox AR. The effect of temperature mismatch on thermoelectric generators electrically connected in series and parallel. Applied Energy. 2014;**123**:47-54. DOI: 10.1016/j.apenergy.2014.02.030

[42] Nour Eddine A, Chalet D, Faure X, Aixala L, Chessé P. Optimization and characterization of a thermoelectric generator prototype for marine engine application. Energy. 2018;**143**:682-695. DOI: 10.1016/j.energy.2017.11.018

[43] Liu X, Li C, Deng YD, Su CQ. An energy-harvesting system using thermoelectric power generation for automotive application. International Journal of Electrical Power & Energy Systems. 2015;**67**:510-516. DOI: 10.1016/j.ijepes.2014.12.045

[44] Fujifilm. Pressure Measurement Film. n.d

[45] Binggeli C. Building Systems for Interior Designers. Hoboken, NJ, USA: John Wiley & Sons, Inc.; 2010

[46] Gorse C, Johnston D, Pritchard M. A Dictionary of Construction, Surveying and Civil Engineering. Oxford University Press; 2012. pp. 440-441. ISBN: 9780199534463

[47] Erica. Nefalit Datasheet 2018. http://www.erica.es/web/carton-fibras/ [Accessed January 31, 2018]

[48] Grupo Flexicel. Flexiband Datasheet 2018. https://www.grupoflexicel.com/pagina.php?id=15008&lang=es [Accessed January 31, 2018]

[49] Rohsenow WM, Hartnett JP, Cho YI. Handbook of Heat Transfer. 3rd ed. New York, United States: McGraw-Hill; 1985

[50] Martínez Echeverri A. Estudio y desarrollo de sistemas termoeléctricos para el aprovechamiento del calor residual en la generación de energía eléctrica. Pamplona, Spain: Universidad Publica de Navarra; 2012